Siberian glaciation as a constraint on Permian–Carboniferous CO_2 levels

William T. Hyde Nicholas School for the Environment and Earth Sciences, Department of Earth and Ocean Sciences, Duke University, Durham, North Carolina 27708, USA
Ethan L. Grossman Department of Geology and Geophysics, Texas A&M University, College Station, Texas 77843, USA
Thomas J. Crowley Nicholas School for the Environment and Earth Sciences, Department of Earth and Ocean Sciences, Duke University, Durham, North Carolina 27708, USA
David Pollard EMS Earth and Environmental Systems Institute, Pennsylvania State University, University Park, Pennsylvania 16802, USA
Christopher R. Scotese Department of Geology, University of Texas at Arlington, Arlington, Texas 76019, USA

ABSTRACT

Reconstructions of Phanerozoic CO_2 levels have generally relied on geochemical modeling or proxy data. Because the uncertainty inherent in such reconstructions is large enough to be climatically significant, inverse climate modeling may help to constrain paleo-CO_2 estimates. In particular, we test the plausibility of this technique by focusing on the climate from 360 to 260 Ma, a time in which the Siberian landmass was in middle to high latitudes, yet had little or no permanent land ice. Our climate model simulations predict a lower limit for CO_2—the value beneath which Siberia acquires "excess" ice. Simulations provide little new information for the period in which Siberia was at a relatively low paleoaltitude (360–340 Ma), but model results imply that paleo-CO_2 levels had to be greater than 2–4× modern values to be consistent with an apparently ice-free Siberia in the late Permian. These results for the later period in general agree with soil CO_2 proxies and the timing of Gondwanan deglaciation, thus providing support for a significant CO_2 increase before the end-Permian boundary event. Our technique may be applicable to other time intervals of unipolar glaciation.

Keywords: paleoclimate, paleoatmosphere, carbon dioxide, glaciation.

INTRODUCTION

The growing body of deep-time paleoclimatic data provides us with a valuable opportunity to test climate models. Those that fail to simulate climates different from the present climate will clearly lack generality; therefore, less confidence can be placed in their predictions of future climate change. Before such tests can be conducted, we need to have a reasonably accurate set of boundary conditions and inputs for the eras in question. It has long been recognized that one of the key inputs is the atmospheric CO_2 level, and considerable progress has been made in reconstructing Phanerozoic CO_2 levels, e.g., geochemical modeling by Berner and Kothavala (2001) and Berner (2006), and by paleosol evidence, e.g., Mora et al. (1996) and Ekart et al. (1999). However, reconstructions of paleo-CO_2 levels are complicated by uncertainties in the underlying data, for example, rates of continental weathering, seafloor spreading, etc. Thus, model predictions such as GEOCARB III in Berner and Kothavala (2001) and GEOCARBSULF in Berner (2006) are necessarily accompanied by large error bars. For example, from the climate modeling point of view, the difference between 2× and 4× CO_2 is very significant.

This sensitivity to CO_2 level leads to the possibility that we may be able to estimate CO_2 through inverse modeling, i.e., we can attempt to determine for a given era just which values of CO_2 reconcile climate model output with some subset of geological data, and then compare this CO_2 prediction with geochemical or other estimates. Consider the question of predicted versus observed ice volumes. Large ice sheets tend to form most easily when summer temperatures are low, which in turn requires both a low average temperature and a weak seasonal cycle (North et al., 1983; Crowley et al., 1986; Hyde et al., 1989). Landmasses with cold average temperatures (e.g., northern Canada) will not sustain permanent ice if a strong seasonal cycle results in a strong summer melt season. However, a small- to medium-sized continent in a high-latitude location will have comparatively cool summers and is particularly likely to be glaciated, and an absence of such glaciation is a strong indicator of high CO_2 levels.

Siberia in the Permian–Carboniferous seems to fulfill these conditions. In this age interval, it was an isolated continent of small to medium size (Fig. 1) and was the northernmost major landmass. Therefore, the condition of an ice-free Siberia may provide a lower boundary for atmospheric CO_2. Evidence from the high northern latitudes in the Permian–Carboniferous is consistent with a transition from a warm climate, in which there was little or no permanent ice (perhaps high-altitude glaciers), to one with extensive seasonal sea ice. Small amounts of permanent ice cannot be ruled out (Crowell, 1999; Zharkov and Chumakov, 2001). For example, in the Sverdrup Basin, Beauchamp (1994) finds a transition from "tropical like" to temperate-warm during the Artinskian (~280 Ma) and a continued cooling to temperate-cold in the Kungarian-Kazanian (~255 Ma). This is consistent with evidence for an increased area of ice-marine deposits on the Kolyma River at this time (Epshteyn, 1981), and cold-water fossils in the Sverdrup Basin and Siberia are overlain in places with Tartarian-stage (~250 Ma) coal beds (Crowell, 1999). There are also Late Permian glacial and glacial-marine sediments amid marine facies in the Kolyma and Okhotsk massifs, and probably in the Verkhoyansk fold belt (Epshteyn, 1973; Chumakov, 1994; Zharkov and Chumakov, 2001). Finally, Hambrey and Harland (1981) argued for a cold climate in northeast Siberia (lower and middle reaches of the Kolyma River) during the Kazanian on the basis of diamictites, which they interpreted as "ice-marine" deposits.

METHODS

The climate–ice-sheet model consists of four submodels that predict ice flow, mass balance, temperature, and bedrock sinking. Ice is assumed to flow subject to a temperature-independent rheology based upon the Nye formulation (Nye, 1959). Precipitation/ablation is computed according to statistical models (Reeh, 1990; Huybrechts and T'Siobbel, 1995), which themselves need inputs of monthly temperatures from a nonlinear, two-dimensional (latitude-longitude), diffusive, seasonal, energy-balanced model (EBM) (Hyde et al., 1989). Bedrock sinking is assumed to occur with a time constant of 4000

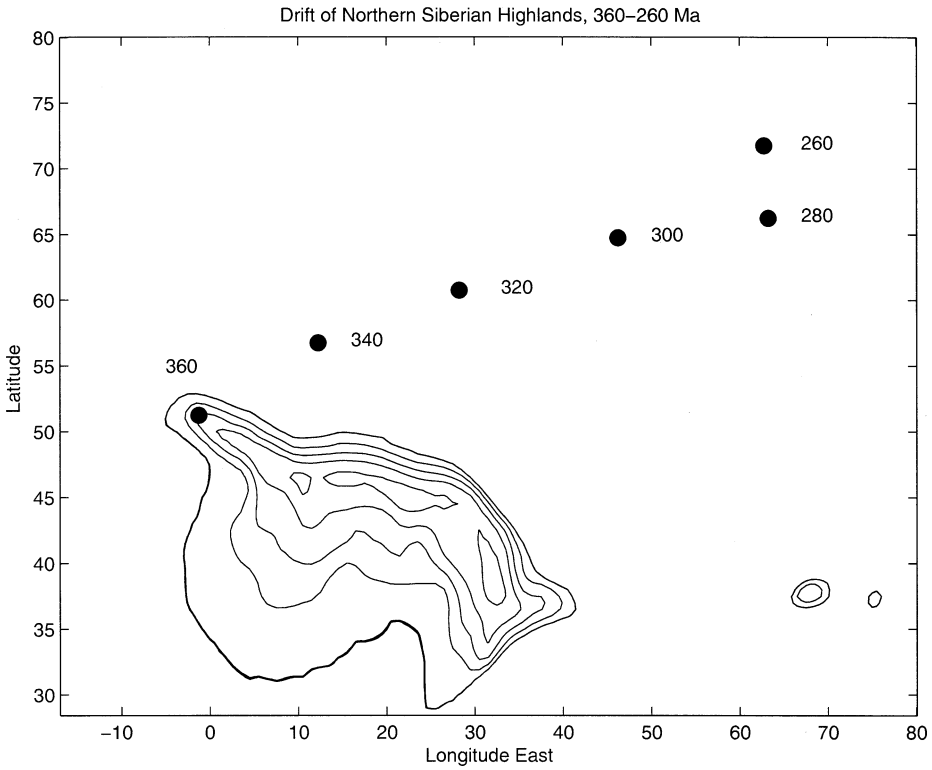

Figure 1. Path of Siberia from 260 to 360 Ma. In early Carboniferous (Mississippian), Siberia was in low mid-latitudes (contoured figure). Over period 360–260 Ma, Siberia drifted northward. Large black dots give northernmost location of Siberian highlands (500 m) over this period. While drift from 340 to 280 Ma was fairly constant, a sharp northward jump occurred between 280 and 260 Ma. This should have encouraged ice-sheet inception. Topographic reconstructions are from Scotese (2001).

yr. For a more complete description of the model, see Tarasov and Peltier (1997). The EBM has been validated against many different global circulation models (GCMs) (Crowley et al., 1991), while the coupled EBM–ice-sheet model has reproduced many features of climate change over the last 120,000 yr and predicts ice for about 80% of the known glacial deposits for the radically different geography of the Carboniferous ice age (Hyde et al., 1999), and has also been applied to Neoproterozoic glaciation (Hyde et al., 2000).

Our strategy is to use this model to simulate Siberian ice for a variety of CO_2 levels every 20 m.y. in our target interval (360–260 Ma), and determine which CO_2 levels are consistent with the geologic evidence for Siberian ice. However, a number of uncertainties must first be considered.

1. Absence of evidence is not evidence of absence. Given the imperfection of the geologic record, it is not reasonable to declare that the evidence demands there be zero ice on Siberia in this interval. For the purposes of this study, we deem any climate with $<1 \times 10^6$ km^3 of ice (approximately one-third the volume of the Greenland ice sheet) to be consistent with the evidence for an ice-free Siberia (we call this the small ice-sheet criterion). An ice sheet of this size would have a negligible effect on sea level, and would probably leave a small glacial geomorphological footprint, which could plausibly have remained undetected, given erosion and burial over the past 300 m.y.

2. Paleotopography is more uncertain than paleogeography, but it is an important boundary condition. High topography allows ice sheets to nucleate in sites that would otherwise be ice free (Hyde et al., 1999). The model allows multiple equilibria—for some boundary conditions, two or more stable climates exist (i.e., with or without an ice sheet). In such a model, a small topographic change may lead to a very different climate (Hyde et al., 1999). However, this is not the case with the small Siberian ice sheets we are considering, because they do not reflect enough sunlight to allow for multiple equilibria (North, 1984). A different mechanism due to the feedback between ice-sheet height and mass balance can also cause multiple equilibria, but this does not seem to occur in the simulations performed in this study. Hence, reasonable changes in Siberian topography should not cause the model to simulate a qualitatively different ice volume.

Given the need for consistency between experiments, we assume zero topography (other than that provided by the ice sheets themselves). In light of this, our CO_2 predictions are minima. We use the paleogeography produced by the Paleomap project (Scotese and Golonka, 1992; Scotese, 1994, 2001), which has an estimated latitudinal error of less than five degrees. We note that this paleogeography is largely consistent with the Permian reconstructions of Ziegler et al. (1997). No attempt is made to model albedo change resulting from different vegetation regimes.

In our target interval, three factors other than CO_2 affect Siberian climate. They are (1) a general northward drift of the landmass as shown in Figure 1, (2) a 1% increase in the solar constant per 100 m.y. (Crowley and Baum, 1992), so that the solar constant grows from 0.964× present value at 360 Ma to 0.974 at 260 Ma, and (3) increased continentality (Scotese, 2001). With time, the first of these factors should favor ice-sheet formation, while the last two should favor ice-free conditions by increasing the average temperature and the seasonality (summer warmth), respectively.

Each of our model runs is 200 k.y. long. For each time slice, we examine the climate response to CO_2 levels ranging from about 0.5× to 12× present, in intervals equal in infrared (IR) forcing to 2.0 W/m^2 (for comparison, the radiative gap between 1× and 2× is ~4 W/m^2). At critical points, where the ice amount changes rapidly with CO_2, we use finer intervals.

In addition to the these changes in CO_2, solar constant, and geography, the model is driven by Milankovitch orbital insolation forcing identical to that which will occur in the next 200 k.y. (Berger, 1978). While we recognize that Milankovitch forcing was different in this era, in some circumstances, orbital change causes ice-sheet initiation, which would not occur for constant orbital parameters (Hyde et al., 1999).

MODEL RESULTS

Our ensemble of experiments produces an array of ice volumes as a function of time and CO_2 level. We show this schematically in Figure 2, where the orange area corresponds to simulations with a vanishingly small amount of ice ($<10^4$ km^3), the gray area to ice volumes of 10^4–10^6 km^3, and the blue areas to ice volumes $>10^6$ km^3. Given our ''small ice-sheet criterion,'' the orange and gray areas are consistent with the evidence for Siberian ice, except possibly at 260 Ma. For reference, we also plot the mean GEOCARB III value (dashed line), as well as the more recent GEOCARBSULF (Berner, 2006) results.

It is clear from this figure that the northward drift of Siberia (Fig. 1) dominates over the increasing solar constant and continentality as a proximal cause for glaciation. Hence, the model requires CO_2 levels to increase with time in order to keep Siberia ice free. This also has the consequence that the area in

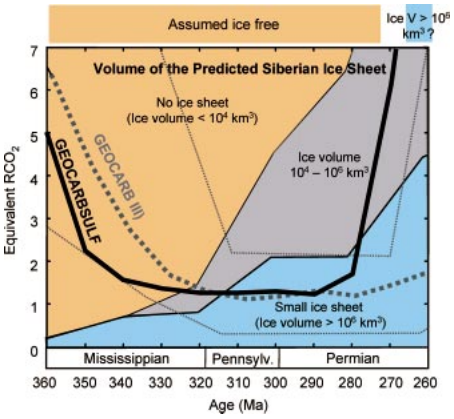

Figure 2. Comparison of predicted Siberian ice regimes with GEOCARB III (dashed line) and GEOCARBSULF (solid line) CO_2 estimates. Early in our target interval, Siberia is far enough south that large ice sheets cannot be grown, except perhaps at unrealistically small CO_2 levels. Hence, our results are consistent with GEOCARB III (Berner, 2001), and we have learned nothing new. In the Permian, however, Siberia's higher latitude results in simulation of substantial ice on Siberia, except for under conditions of very high CO_2 levels. Upper and lower GEOCARB III error bars are plotted for reference. Time scale is from Gradstein et al. (2005). V—volume; RCO_2—ratio of CO_2 to the preindustrial value.

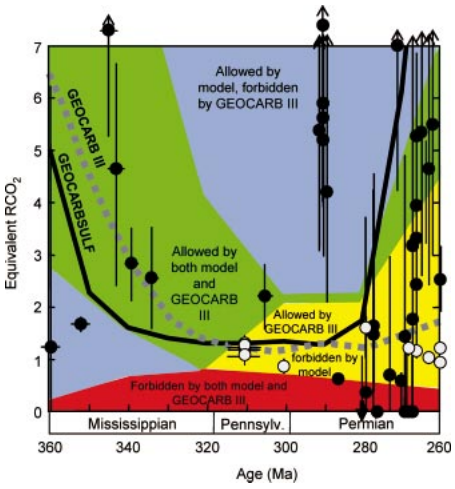

Figure 3. Confidence limits on GEOCARB III and model's predicted 1 × 10^6 km^3 ice-volume line can be used to divide (time, CO_2) plane into a number of regions. Red region represents CO_2 levels that are both below lower confidence limit of GEOCARB III and for which model predicts an ice sheet too large to be compatible with Siberian geology. Yellow region consists of CO_2 levels that are compatible with GEOCARB III but not with model results. Green areas are compatible with both, and blue regions have CO_2 levels that are compatible with model, but lie outside GEOCARB III limits. Circa 260 Ma, Siberia might have supported more land ice than our horizon of 10^6 km^3. If so, our inverse modeling results will allow a lower CO_2 level at that time. Time scale is from Gradstein et al. (2005). We also compare our phase domains with paleo-CO_2 reconstructions compiled in Royer et al. (2004). RCO_2—ratio of CO_2 to the preindustrial value.

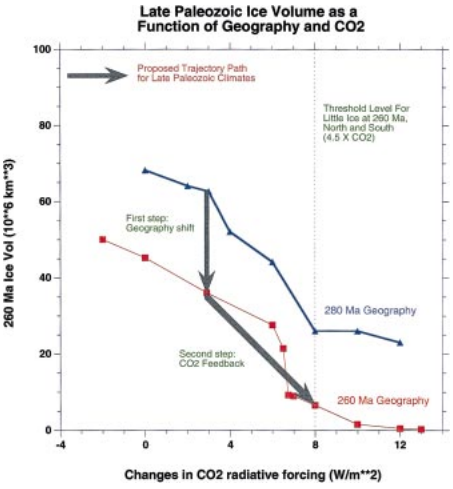

Figure 4. Calculated Gondwanan ice volume as a function of paleogeography and CO_2 level for 280 and 260 Ma. A substantial Gondwanan ice sheet is consistent with CO_2 levels in green zone of Figure 3 at 280 Ma, while at 260 Ma, the ice sheet is largely eliminated by CO_2 levels in upper third of GEOCARB III range. Arrows suggest a trajectory path for deglaciation—a northward movement of landmasses causing initial melting followed by a suggested CO_2 feedback (of unspecified origin).

RCO_2 (ratio of CO_2 to the preindustrial value) space, in which ice is within the range 10^4–10^6 km^3, increases with time. This is due to the saturation of the CO_2 bands represented in the logarithmic relation between radiative forcing and CO_2 in Myhre et al. (1998). Thus, the intermediate low-ice state (gray in Fig. 2) broadens as Siberia drifts northward.

As GEOCARBSULF predicts a generally declining level of atmospheric CO_2 with time in the Permian–Carboniferous, our small ice-sheet line eventually rises above the mean GEOCARBSULF prediction, indicating disagreement. However, geochemical predictions have an inherent uncertainty. The true level of agreement or disagreement between the model and the older GEOCARB III results is revealed in Figure 3. In this figure, we plot the various intersection sets between the ice-volume regimes predicted by the model (Fig. 2) and the swath allowed by the GEOCARB III results, including error bars.

Barring some uncertainty at 260 Ma, the green zone in Figure 3 corresponds to levels of CO_2 that satisfy both GEOCARB III and the model's small ice-sheet criterion. The blue zone is allowed by the model but forbidden by GEOCARB III, the yellow zone is forbidden by the model but allowed by GEOCARB III, while CO_2 values in the red area are forbidden by both. Our green zone also displays a considerable degree of concordance with other paleo-CO_2 reconstructions, e.g., Royer et al. (2004), as summarized in Figure 3.

The location of the allowed zone in our model obviously depends on our small ice-sheet criterion. A more stringent criterion ($<10^4$ km^3 of ice) has a negligible effect at 360 and 340 Ma, but a progressively larger one until more than 8× CO_2 is required at 260 Ma (Fig. 2). Allowing double the ice of our criterion naturally lowers the minimum allowed CO_2 level, but by $<1/2\times$ CO_2. This widens the zone of agreement between the model and GEOCARB III.

For the earlier part of the Carboniferous, 360 and 340 Ma, our inverse method supplies no new information. Siberia lies far enough south that even CO_2 levels much lower than those predicted by GEOCARBSULF or other paleoreconstructions are consistent with an ice-free Siberia. Even given substantial topography on Siberia, this conclusion is unlikely to change significantly, with only the lower range of the Royer et al. (2004) composite likely to be inconsistent with model results (Fig. 3).

Near 320 Ma, the model's lower limit agrees closely with that of GEOCARBSULF and is also consistent with other paleoreconstructions. At 300 Ma, the model agrees only with the extreme upper limit of the GEOCARB III results, while at 280 Ma, it seems to be in agreement with the new GEOCARBSULF predictions, but not with the GEOCARB III results. For these latter times, the model is also in agreement with the results of Tabor et al. (2004) and Royer et al. (2004) (Fig. 3), which suggest somewhat higher CO_2 levels.

For 260 Ma, the assumption of no large ice sheet on Siberia also results in good agreement with the GEOCARBSULF results. However, there is more evidence for Siberian ice at this time, so our small ice-sheet criterion may not hold. The evidence for ice is sparse enough that it does not seem probable that the ice sheet was very large, but if the Siberian ice sheet at 260 Ma were as large as 2 × 10^6 km^3, the climate model would agree with the middle range of the GEOCARB III estimates for this period. The lower GEOCARB III estimates would result in ice sheets that appear to be too large (~6 × 10^6 km^3 for present CO_2), as would the Beerling (2002) proxy estimates. While our intent in this paper is to focus on Siberia, the model's predictions of Gondwanan ice (Fig. 4) provide a consistency check on our results. Note that the northward movement of the entire Pangean landmass after 280 Ma was associated with a decrease in ice cover on Gondwana. However, CO_2 feedbacks would have to be invoked to boost levels from about 1.8× to 4.5× CO_2 (~480–1260 ppm)—enough to preclude significant ice cover in both north and south. R.A. Berner

(2005, personal commun.) states that no reasonable combination of parameters allows GEOCARBSULF to predict more than ~4× CO_2 in this interval.

The agreement in the Late Permian with GEOCARBSULF (but not with GEOCARB III) is perhaps the most interesting result we obtained. The model also agrees with much of the soil proxy CO_2 data, but not with the stomata proxy CO_2 data. High CO_2 levels for this time are also required for the massive melt back of Gondwanan ice cover in the Sakmarian at ~270 Ma, e.g., Crowley and Baum (1992), Ziegler et al. (1997), Crowell (1999), and Hyde et al. (1999). Part (or all) of the stomatal data discrepancy could reflect the time scale used in various proxy CO_2 data sets, as shown by Royer (2006), who demonstrated that putting all data on a uniform time scale supports the interpretation of higher CO_2 levels before the end of the Permian, which is in agreement with our results.

CONCLUSIONS

In this paper, we have shown how an inverse modeling technique involving predictions of ice volume can be used as a constraint on paleo-CO_2 values. We have applied the technique to the question of Permian–Carboniferous Siberian ice volume, with the result that the model agrees with the new GEOCARBSULF results (except at 300 Ma), but not with the earlier GEOCARB III predictions. For the interval 300–280 Ma, 2× present CO_2 allows the existence of a substantial Gondwanan ice sheet. Constraints due to the presence or absence of ice for both Siberia and Gondwana, combined with new analyses and models, thus may provide a consistent view of high CO_2 levels before the end-Permian event. Our technique should be applicable to other times, particularly those that have small, ice-free continents at high latitudes.

ACKNOWLEDGMENTS

This work was supported by National Science Foundation (NSF) grant EAR-0003596 (Grossman and Hyde), the Mollie B. and Richard A. Williford Professorship (Texas A&M University), and by NSF grants to Hyde and Crowley.

REFERENCES CITED

Beauchamp, B., 1994, Permian cooling in the Canadian Arctic, *in* Klein, G.D., ed., Pangea: Paleoclimates, tectonics, and sedimentation during accretion, zenith and breakup of a supercontinent: Geological Society of America Special Paper 288, p. 229–246.

Beerling, D.J., 2002, Low atmospheric CO_2 levels during the Permo-Carboniferous glaciation inferred from fossil lycopsids: Proceedings of the National Academy of Sciences of the United States of America, v. 99, p. 12,557–12,571.

Berger, A., 1978, Long-term variations of daily insolation and Quaternary climate changes: Journal of Atmospheric Sciences, v. 35, p. 2362–2367, doi: 10.1175/1520-0469(1978)035<2362:LTVODI>2.0.CO;2.

Berner, R.A., 2006, GEOCARBSULF: A combined model for Phanerozoic atmospheric O_2 and CO_2 over Phanerozoic time: American Journal of Science, v. 301, p. 182–204.

Berner, R.A., and Kothavala, Z., 2001, GEOCARB III; A revised model of atmospheric CO_2 over Phanerozoic time: American Journal of Science, v. 301, p. 182–204.

Chumakov, N.M., 1994, Evidence of Late Permian glaciation in the Kolyma river basin: A repercussion of the Gondwanan glaciation in northeast Asia?: Stratigrafiya, Geologicheskaya, Korrelyatsiya, v. 2, p. 130–150.

Crowell, J.C., 1999, Pre-Mesozoic ice ages: Their bearing on understanding the climate system: Geological Society of America Memoir 192, 112 p.

Crowley, T.J., and Baum, S.K., 1992, Modeling late Paleozoic glaciation: Geology, v. 20, p. 507–510, doi: 10.1130/0091-7613(1992)020<0507:MLPG>2.3.CO;2.

Crowley, T.J., Short, D.A., Mengel, J.G., and North, G.R., 1986, Role of seasonality in the evolution of climate over the past 100 million years: Science, v. 231, p. 579–584.

Crowley, T.J., Baum, S.K., and Hyde, W.T., 1991, Climate model comparisons of Gondwanan and Laurentide glaciations: Journal of Geophysical Research, v. D5, p. 9217–9226.

Ekart, D.D., Cerling, T., Montanez, I., and Tabor, N.J., 1999, A 400 million year carbon isotope record of pedogenic carbonate: Implications for paleoatmospheric carbon dioxide: American Journal of Science, v. 299, p. 805–827.

Epshteyn, O.G., 1973, Lithology and formation conditions of Upper Permian glacial-marine sediments in the Southern Yana-Kolyma folded region [dissertation]: Central Geological expedition, Magadan.

Epshteyn, O.G., 1981, Middle Carboniferous ice-marine deposits of the northeastern USSR, *in* Hambrey H.A., and Harland, W.B., eds., Earth's pre-Pleistocene glacial record: Cambridge, Cambridge University Press, p. 270–273.

Gradstein, F.M., and 21 other, 2005, A geologic time scale 2004: Cambridge, Cambridge University Press, p. 268–269.

Hambrey, H.A., and Harland, W.B., eds., 1981, Earth's pre-Pleistocene glacial record: Cambridge, Cambridge University Press, 1004 p.

Huybrechts, P., and T'Siobbel, S., 1995, Thermomechanical modelling of Northern Hemisphere ice sheets with a two-level mass-balance parameterization: Annals of Glaciology, v. 21, p. 111–116.

Hyde, W.T., Crowley, T.J., Kim, K.-Y., and North, G.R., 1989, Comparison of GCM and energy balance model simulations of seasonal temperature changes over the past 18,000 years: Journal of Climate, v. 2, p. 864–887, doi: 10.1175/1520-0442(1989)002<0864:COGAEB>2.0.CO;2.

Hyde, W.T., Crowley, T.J., Tarasov, L., and Peltier, W.R., 1999, The Pangean ice age: Studies with a coupled climate-ice sheet model: Climate Dynamics, v. 15, p. 619–629, doi: 10.1007/s003820050305.

Hyde, W.T., Crowley, T.J., Baum, S.K., and Peltier, W.R., 2000, Neoproterozoic 'snowball Earth' simulations with a coupled climate/ice-sheet model: Nature, v. 405, p. 425–429, doi: 10.1038/35013005.

Mora, C.I., Dreise, S.G., and Colarusso, L.A., 1996, Middle to late Paleozoic atmospheric CO_2 levels from soil carbonate and organic matter: Science, v. 271, p. 1105–1107.

Myhre, G., Highwood, E.J., Shine, K.P., and Stordal, F., 1998, New estimates of radiative forcing due to well-mixed greenhouse gases: Geophysical Research Letters, v. 25, p. 2715–2718, doi: 10.1029/98GL01908.

North, G.R., 1984, The small ice cap instability in diffusive climate models: Journal of Atmospheric Sciences, v. 41, p. 3390–3395, doi: 10.1175/1520-0469(1975)032<1301:ASTASC>2.0.CO;2.

North, G.R., Mengel, J.G., and Short, D.A., 1983, Simple energy balance model resolving the seasons and continents: Application to the astronomical theory of the ice ages: Journal of Geophysical Research, v. 99, p. 6576–6658.

Nye, J.F., 1959, The motion of ice sheets and glaciers: Journal of Glaciology, v. 3, p. 493–507.

Reeh, N., 1990, Parameterization of melt rate and surface temperature on the Greenland ice sheet: Polarforschung, v. 59, no. 3, p. 113–128.

Royer, D.L., 2006, CO_2-forced climate thresholds during the Phanerozoic: Geochimica et Cosmochimica Acta, v. 70. (in press).

Royer, D.L., Berner, R.A., Montanez, I.P., Tabor, N., and Beerling, D.J., 2004, CO_2 as a primary driver of Phanerozoic climate change: GSA Today, v. 14(3), p. 4–10, doi: 10.1130/1052-5173(2004)014<4:CAAPDO>2.0.CO;2.

Scotese, C.R., 1994, Late Carboniferous paleogeographic map, *in* Klein, G.D., ed., Pangea: Paleoclimates, tectonics, and sedimentation during accretion, zenith and breakup of a supercontinent: Geological Society of America Special Paper 288, p. 5–9.

Scotese, C.R., 2001, Atlas of Earth history, Volume I. Paleogeography: Arlington, University of Texas, Paleomap project, 52 p.

Scotese, C.R., and Golonka, J., 1992, Paleogeographic atlas: Arlington, University of Texas, Paleomap project, 34 p.

Tabor, N.J., Yapp, C.J., and Montanez, I.P., 2004, Goethite, calcite, and organic matter from Permian and Triassic soils: Carbon isotopes and CO_2 concentrations: Geochimica et Cosmochimica Acta, v. 68, p. 1503–1517, doi: 10.1016/S0016-7037(03)00497-6.

Tarasov, L., and Peltier, W.R., 1997, Terminating the 100 kyr ice age cycle: Journal of Geophysical Research, v. 102(D18), p. 21,665–21,693, doi: 10.1029/97JD01766.

Zharkov, M.A., and Chumakov, N.M., 2001, Paleogeography and sedimentation settings during Permian-Triassic reorganizations in biosphere: Stratigrafiya, Geologicheskaya, Korrelyatsiya, v. 9, p. 340–363.

Ziegler, A.M., Hulver, M.L., and Rowley, D.B., 1997, Permian world topography and climate, *in* Martini, I.P., ed., Late glacial and postglacial environmental changes–Quaternary, Carboniferous-Permian and Proterozoic: New York, Oxford University Press, p. 111–146.

Manuscript received 19 September 2005
Revised manuscript received 5 January 2006
Manuscript accepted 11 January 2006

Printed in USA